Multi-Time Simulation of Voltage-Controlled Oscillators

Onuttom Narayan[*]   Jaijeet Roychowdhury[†]

Abstract

We present a novel formulation, called the WaMPDE, for solving systems with forced autonomous components. An important feature of the WaMPDE is its ability to capture frequency modulation (FM) in a natural and compact manner. This is made possible by a key new concept: that of *warped time*, related to normal time through separate time scales. Using warped time, we obtain a completely general formulation that captures complex dynamics in autonomous nonlinear systems of arbitrary size or complexity. We present computationally efficient numerical methods for solving large practical problems using the WaMPDE. Our approach explicitly calculates a time-varying local frequency that matches intuitive expectations. Applied to VCOs, WaMPDE-based simulation results in speedups of two orders of magnitude over transient simulation.

1 Introduction

Oscillatory behaviour is ubiquitous in nature and can be found in a variety of electrical, mechanical, gravitational and biological systems. In electronics, for example, self-oscillation manifests itself in voltage-controlled oscillators (VCOs), phase-locked loops (PLLs), frequency dividers, $\Sigma\Delta$ modulators, etc.. In the presence of external forcing, these systems can exhibit complex dynamics, such as frequency modulation (FM), entrainment or mode locking, period multiplication and chaos. Despite their universality, it is difficult to predict the response of a general autonomous system in a satisfactory and reliable manner.

In this paper, we present the WaMPDE (**Wa**rped **M**ultirate **P**artial **D**ifferential **E**quation), a new approach for analysing a large class of forced and unforced oscillatory systems. The approach is particularly useful for oscillators exhibiting FM. Conventional methods, discussed in Section 2, are typically error-prone and computationally intensive for oscillators in general, and especially for forced ones exhibiting FM-quasiperiodicity.

A key aspect of our methods is a compact representation of FM signals using functions of several time variables, some of which are "warped". The essence of the time-warping concept is to take an FM signal and stretch or squeeze the time axis by different amounts at different times in order to make the density of the signal undulations uniform. The variation of this stretching is much slower than the undulations themselves, hence a multiple time approach is used to separate the time scales. An important feature of the WaMPDE is that, unlike previous methods, it automatically and explicitly determines the local frequency as it changes with time (see Section 3). Further, our approach also eliminates the problem of growing phase error that limits previous numerical techniques for oscillators. AM-quasiperiodicity, mode-locking, period multiplication, etc., emerge naturally as special cases.

Numerical computations for the WaMPDE can be performed using time-domain or frequency-domain methods, or combinations. In particular, existing codes for previous methods like the MPDE and harmonic balance (see Section 2) can be modified easily to perform WaMPDE-based calculations. The use of iterative linear techniques [Saa96] enables large systems to be handled efficiently.

[*]University of California, Santa Cruz.
[†]Bell Laboratories, Murray Hill.

The remainder of this paper is organized as follows. Section 2 contains a brief review of previous work. Section 3 is a tutorial-style exposition of the main concepts of the WaMPDE formulation, the mathematical details of which are presented in Section 4. In Section 5, the new methods are applied to practical VCO circuits and compared against existing techniques.

2 Previous Work

A vast literature is available on oscillator design and analysis; here we provide only a few references representative of different approaches. Many previous analyses of oscillators are from a practical design perspective; these investigations typically apply purely linear concepts (e.g., [Ven82, Par83, Roh97, Got97]) to obtain simple design formulae. However, linear models are not even qualitatively adequate for practical oscillators, since nonlinearity is essential for orbital stability (see, e.g., [Far94]). Nonlinear analyses have largely been of polynomially-perturbed linear oscillators [vdP22, Hay64, KC81, Mur91, Far94], with sophisticated studies focussing typically on mode locking and transitions to chaos [Lor63, PC89, NB95]. Relatively little attention has been paid to phenomena like FM-quasiperiodicity, even though they are of great importance in communication applications.

A previous analytical technique with similarities to our present approach is the multiple-variable expansion procedure (e.g., [KC81]), useful for simple harmonic oscillators with small nonlinear perturbations and without external forcing. The dependence on the strength of the nonlinearity is typically different in different parts of the solution, and multiple time variables have to be introduced to obtain a tractable perturbation theory. Unfortunately, the method is intrinsically a perturbation approach, and even convergence of the solution series is not guaranteed[1].

For real oscillators, as for most complex systems, numerical simulation has been the predominant means of predicting detailed responses. Simulation of oscillators, however, presents unique difficulties absent in non-autonomous systems. A fundamental problem is the intrinsic phase-instability of oscillators, *i.e.*, the absence of a time reference. As a result, numerical errors grow and phase error increases unboundedly in the course of numerical ODE solution. For unforced oscillators in periodic steady state, boundary-value methods such as shooting [AT72, Ske80, NB95, TKW95] and harmonic balance [NV76, Haa88, RN88, GS91, Mar92, MFR95] can be used to obtain both the time period and the steady-state solution. Neither shooting nor harmonic balance can be applied, however, to forced oscillators with FM-quasiperiodic responses, as they require an impractically large number of time-steps or variables (see Section 3). In practice, the separation of the time scales is often reduced artificially to make the problem tractable. As illustrated in Section 5, such ad-hoc approaches can lead to qualitatively misleading results.

The warped-time approach presented in this paper is a generalization of a recent multi-time approach (the Multirate Partial Differential Equation (MPDE) [BWLBG96, Roy97, Roy99]) for non-autonomous systems with widely separated time scales. Earlier efforts at generalizing the MPDE to autonomous systems [BL98] used non-rectangular boundaries to capture frequency variation. It has been shown ([Roy99]), however, that this approach is limited to oscillations that eventually become periodic, and cannot, for instance, accommodate FM-quasiperiodicity.

3 Essential concepts

In this section, we introduce several concepts at the core of this work. We first review why it is advantageous to use two or more time scales for analysing quasiperiodic signals, using amplitude-modulated (AM) signals for illustration. Then we show that although frequency-modulated (FM) signals can be quasiperiodic, the multi-time ap-

---

[1]The method relies on asymptotic expansions, which in general are not convergent.
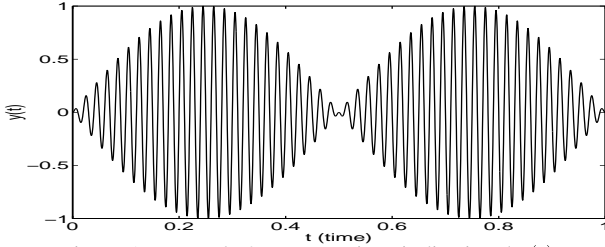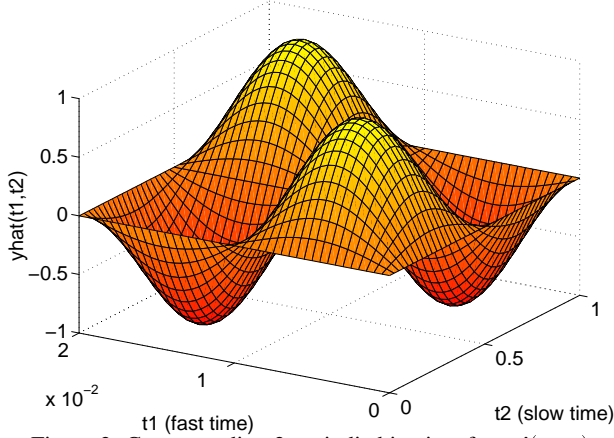
Figure 1: Example 2-tone quasi-periodic signal $y(t)$

Figure 2: Corresponding 2-periodic bivariate form $\hat{y}(t_1, t_2)$

t2

Figure 3: Path in the t_1-t_2 plane

Note that $\hat{y}(t_1, t_2)$ is periodic with respect to both t_1 and t_2, *i.e.*, $\hat{y}(t_1 + T_1, t_2 + T_2) = \hat{y}(t_1, t_2)$. The plot of $\hat{y}(t_1, t_2)$ on the rectangle $0 \leq t_1 \leq T_1$, $0 \leq t_2 \leq T_2$ is shown in Figure 2. Because $\hat{y}$ is bi-periodic, this plot repeats over the rest of the t_1-t_2 plane. Note also that $\hat{y}(t_1, t_2)$ does not have many undulations, unlike $y(t)$ in Figure 1. *Hence it can be represented by relatively few points, which, moreover, do not depend on the relative values of T_1 and T_2, unlike Figure 1.* Figure 2 was plotted with 225 samples on a uniform 15×15 grid – three times fewer than for Figure 1. This saving increases with increasing separation of the periods T_1 and T_2.

Note further that it is easy to recover $y(t)$ from $\hat{y}(t_1, t_2)$, simply by setting $t_1 = t_2 = t$, and using the fact that $\hat{y}$ is bi-periodic. Given any value of t, the arguments to $\hat{y}$ are given by $t_i = t \bmod T_i$. For example:

$$
\begin{aligned}
y(1.952\text{s}) &= \hat{y}(1.952\text{s}, 1.952\text{s}) \\
&= \hat{y}(97T_1 + 0.012\text{s}, T_2 + 0.952\text{s}) \\
&= \hat{y}(0.012\text{s}, 0.952\text{s})
\end{aligned}
$$

Given $\hat{y}(t_1, t_2)$, it is easy to visualise what $y(t)$ looks like. As t increases from 0, the path given by $\{t_i = t \bmod T_i\}$ traces the sawtooth path shown in Figure 3. By noting how $\hat{y}$ changes as this path is traced in the t_1-t_2 plane, $y(t)$ can be visualised. *When the time-scales are widely separated, therefore, inspection of the bivariate waveform directly provides information about the slow and fast variations of $y(t)$ more naturally and conveniently than $y(t)$ itself.*

The above discussion has illustrated two important features: 1. *the bivariate form can require far fewer points to represent numerically than the original quasiperiodic signal*, yet 2. *it contains all the information needed to recover the original signal completely.* These concepts are the key to the MPDE approach [BWLBG96, Roy97, Roy99] for analysing non-autonomous systems. The basic notion is to solve directly for the compact multivariate forms of a DAE's solution. To achieve this, the DAE is replaced by a closely related partial differential equation called the MPDE. By applying boundary conditions to the MPDE and solving it with numerical methods, the multivariate solutions are obtained efficiently. The univariate solution of the original DAE can be easily computed from the multivariate solution of the MPDE; often, however, information of interest can be obtained directly by inspecting the multivariate solution. We refer the reader to [Roy99, Roy97] for further details.

When the DAEs under consideration contain autonomous components, FM-quasiperiodicity can be generated. FM cannot, in general, be represented compactly as in Figure 2. We illustrate the difficulty with an example. Consider the following prototypical FM signal:

$$ x(t) = \cos\left(2\pi f_0 t + k\cos(2\pi f_2 t)\right), \qquad f_0 \gg f_2 \qquad (3) $$

with instantaneous frequency

$$ f(t) = f_0 - k f_2 \sin(2\pi f_2 t). \qquad (4) $$

$x(t)$ is plotted in Figure 4 for $f_0 = 1\text{MHz}$, $f_2 = 20\text{KHz}$, and modulation index $k = 8\pi$. Following the same approach as for (1), a bivariate form can be defined to be

$$ \hat{x}_1(t_1, t_2) = \cos\left(2\pi f_0 t_1 + k\cos(2\pi f_2 t_2)\right), \quad \text{with } x(t) = \hat{x}_1(t, t). \quad (5) $$

Note that $\hat{x}_1$ is periodic in t_1 and t_2, hence $x(t)$ is quasiperiodic with frequencies f_0 and f_2. Unfortunately, $\hat{x}_1(t_1, t_2)$, illustrated in Figure 5, is not a simple surface with only a few undulations like Figure 2. When $k \gg 2\pi$, i.e., $k \approx 2\pi m$ for some large integer m, then $\hat{x}_1(t_1, t_2)$ will undergo about m oscillations as a function of t_2 over one period T_2. In practice, k is often of the order of $\frac{f_0}{f_2} \gg 2\pi$, hence this number of undulations can be very large. Therefore it becomes difficult to represent $\hat{x}_1$ efficiently by sampling on a two-dimensional grid. It is also clear, from Figure 5, that representing (3) in the frequency domain will require a large number of Fourier coefficients to capture the undulations.

proaches that work for AM (or immediate extensions thereof) do not confer the same advantages. Next, we introduce the concept of warped time and show how it can be used to remedy the situation for FM. We discuss the important issue of ambiguities in the concept of local frequency, and show how to obtain a useful definition that is consistent with intuition. Finally, as a prelude to Section 4, we outline the basic features of the WaMPDE.

Consider the waveform $y(t)$ shown in Figure 1, a simple two-tone quasiperiodic signal given by:

$$ y(t) = \sin\left(\frac{2\pi}{T_1}t\right)\sin\left(\frac{2\pi}{T_2}t\right), \qquad T_1 = 0.02\text{s}, \quad T_2 = 1\text{s} \quad (1) $$

The two tones are at frequencies $f_1 = \frac{1}{T_1} = 50\text{Hz}$ and $f_2 = \frac{1}{T_2} = 1\text{Hz}$, *i.e.*, there are 50 fast-varying sinusoids of period $T_1 = 0.02\text{s}$ modulated by a slowly-varying sinusoid of period $T_2 = 1\text{s}$. Such multi-rate waveforms, *i.e.*, with two or more "components" varying at widely separated rates, arise in many practical situations, including oscillators, mixers, switched-capacitor filters, planetary systems, combustion engines, etc..

When such signals result from differential-algebraic equation (DAE) systems being solved by numerical integration (*i.e.*, transient simulation), the time-steps taken need to be spaced closely enough that each rapid undulation of $b(t)$ is sampled accurately. If each fast sinusoid is sampled at n points, the total number of time-steps needed for one period of the slow modulation is $n\frac{T_2}{T_1}$. To generate Figure 1, 15 points were used per sinusoid, hence the total number of samples was 750. This number can be much larger in applications where the rates are more widely separated, e.g., separation factors of 1000 or more are common in electronic circuits. Also, while the particular $b(t)$ in (1) can be compactly represented in the frequency domain with only two Fourier components, the same is not true for, e.g., the product of a sine wave and a square wave. Hence frequency-domain representations do not, in general, solve the problem of inefficient numerical representation of multi-rate signals.

Now consider a multivariate representation of $y(t)$, obtained as follows: for the 'fast-varying' parts of $y(t)$, t is replaced by a new variable t_1; for the 'slowly-varying' parts, by t_2. The resulting function, now of two variables, is denoted by $\hat{y}(t_1, t_2)$:

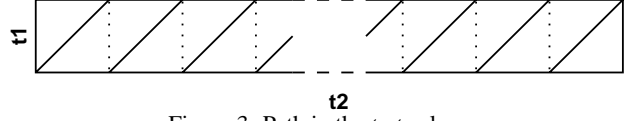$$ \hat{y}(t_1, t_2) = \sin\left(\frac{2\pi}{T_1}t_1\right)\sin\left(\frac{2\pi}{T_2}t_2\right) \qquad (2) $$
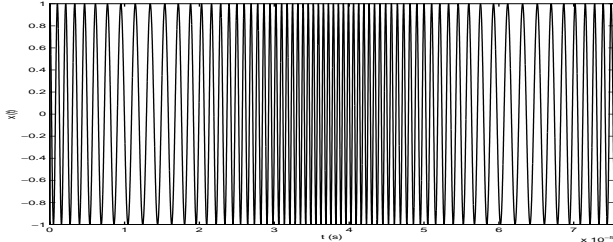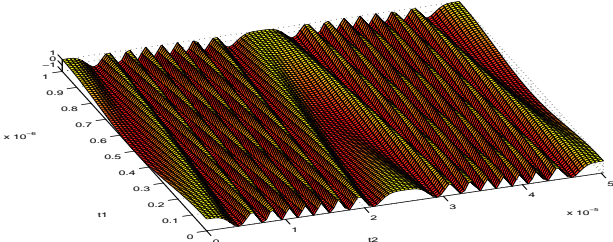
Figure 4: FM signal

Figure 5: $\hat{x}_1$: unwarped bivariate representation of FM signal

A plausible approach towards resolving this representation problem is based on the intuition that FM is a slow change in the instantaneous frequency of a fast-varying signal. In the multivariate representation (2), the high-frequency component is the inverse of T_1, the time-period along the t_1 (fast) time axis. It is natural to hope, therefore, that FM solutions can be captured by making this time-period change along the slow time axis t_2, *i.e.*, change T_1 to a periodic function $T_1(t_2)$, itself periodic with period T_2. Unfortunately, it can be shown ([Roy99]) that FM-quasiperiodicity in a DAE *cannot* be captured by making T_1 a function of t_2.[2] It is easy to see qualitatively why this is the case. Although Figures 2 and 5 show the signal over only one period in each of the two time directions, the bivariate form is actually periodic over the entire t_1-t_2 plane. However, making the time-period T_1 a function $T_1(t_2)$ turns the rectangular domain $[0, T_1] \times [0, T_2]$ (of Figures 2 and 5) into a non-rectangular domain of variable width. While it is possible to obtain a periodic function on the t_1-t_2 plane by placing rectangular boxes side by side to tile the entire plane, it is obvious that this cannot be done with boxes of variable width.

The WaMPDE approach of this work resolves this problem by preserving the rectangular shape of the domain boxes, and bending the path along which $y(t)$ is evaluated away from the diagonal line shown in Figure 3, so that its slope changes slowly. Since along the bent path $t_2 = t$, but t_1 is no longer equal to t, we refer to t_1 as a warped time-scale. As mentioned in Section 1, this effectively results in stretching and squeezing the time axis differently at different times to even out the period of the fast undulations.

We illustrate this by returning to (3). Consider the following new multivariate representation

$$\hat{x}_2(\tau_1, \tau_2) = \cos(2\pi\tau_1) \qquad (6)$$

together with the warping function

$$\phi(\tau_2) = f_0\tau_2 + \frac{k}{2\pi}\cos(2\pi f_2\tau_2). \qquad (7)$$

We now retrieve our one-dimensional FM signal (i.e., (3)) as

$$x(t) = \hat{x}_2(\phi(t), t). \qquad (8)$$

Note that both $\hat{x}_2$ and ϕ, given in (6) and (7), can be easily represented with relatively few samples, unlike $\hat{x}_1$ in (5). Note further that $\phi(t)$ is the sum of a linearly increasing term and a periodic term, hence its derivative is periodic. This periodic derivative is equal to the instantaneous frequency, given in (4), of $x(t)$. We will elaborate further on the significance of $\frac{\partial\phi}{\partial t}$ shortly.

It is apparent that there is no unique bivariate form and warping function satisfying (8) – for example, two representations $\hat{x}_1$ and $\hat{x}_2$ have already been given (the warping function for $\hat{x}_1$ is $\phi(t) = t$).

---

[2]Nevertheless, Brachtendorf [BL98] has shown that this concept can be used to analyse transients in the special case of oscillators that eventually become T_1-periodic.
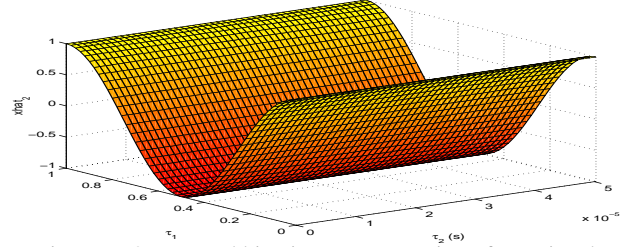

Figure 6: $\hat{x}_2$: warped bivariate representation of FM signal

More generally, any warping function can be chosen, but at the possible cost of a resulting bivariate representation that cannot be sampled efficiently. To find an efficient bivariate representation, a crucial step in our approach is to avoid specifying the function $\phi(t)$ *a priori*, but to impose a smooth "phase" condition instead on the bivariate function, and use this to calculate ϕ. The phase condition can, for instance, require that the phase of the τ_1-variation of the function should vary only slowly (or not at all) as τ_2 is changed. Alternatively, a time-domain condition on the bivariate function (or a derivative) can be specified. As an illustration, consider the requirement that the τ_1-derivative along the line $\tau_1 = 0$ be a slowly-varying function of τ_2:

$$\frac{\partial\hat{x}_3(0, \tau_2)}{\partial\tau_1} = -2\pi\sin(2\pi f_2\tau_2) \qquad (9)$$

together with

$$\hat{x}_3(\phi_3(t), t) = x(t) = \cos\left(2\pi f_0 t + k\cos(2\pi f_2 t)\right). \qquad (10)$$

As is easily verified, these conditions lead to the following solutions for $\hat{x}_3$ and ϕ_3:

$$\hat{x}_3(\tau_1, \tau_2) = \cos(2\pi\tau_1 + 2\pi f_2\tau_2)$$
$$\phi_3(t) = f_0 t + \frac{k}{2\pi}\cos(2\pi f_2 t) - f_2 t \qquad (11)$$

Although $\hat{x}_3$ and ϕ_3 are not identical to $\hat{x}_2$ and ϕ in (6) and (7), they retain the desired property of being easy to sample.

When $\hat{x}_2$ and ϕ in (6) and (7) are chosen to be the warped bivariate representation of $x(t)$, the instantaneous frequency in (4) is the derivative of $\phi(t)$, as already noted. The derivative of $\phi_3(t)$, on the other hand, differs from the instantaneous frequency by the constant $-f_2$. In general, all choices of $\phi(t)$ that result in compact representations will differ in their derivatives $\frac{\partial\phi}{\partial t}$ by amounts only of the order of the slow frequency f_2. When the fast frequency is much greater than the slow one, this difference is small compared to the instantaneous frequency in (4), therefore the term *local frequency* for $\frac{\partial\phi}{\partial t}$ is justified. The utility of the local frequency is that it is well-defined for *any* FM signal (possibly with non-sinusoidal waveforms and varying amplitudes), not just the ideal one of (3), yet retains the essential intuition of FM. The ambiguity in $\frac{\partial\phi}{\partial t}$, of order f_2, is quite reasonable, since the intuitive concept of frequency is only meaningful to the same order. It should be kept in mind, of course, that concepts of varying frequency make intuitive sense only when the fast and slow time scales are widely separated.

The time warping concept can also be understood in a different, visual, manner. The difficulty in using $\hat{x}_1$ of (5) is due to the fact that changing t_2 by even a small amount results in a large change in the phase of the outer cosine function, because k is large. Thus the function is the same on all lines parallel to the t_1 axis, except for a phase that differs substantially for even lines that are nearby. The representation problem that this causes can be dealt with by sliding these lines up and down in the t_1 direction till there is no variation (or slow variation) in the phase from one line to another. This results in changing the rectangular domain box of Figure 2 to a non-rectangular one, but whose width is *constant* (*i.e.* with curved but parallel boundaries). In addition, the straight-line $t_1 = t_2$ path changes to a curved path because of the phase adjustment. The doubly periodic bivariate representation can be obtained by tiling the t_1-t_2 plane with the curved domain boxes (possible because the width is constant); in fact, after extending the function to the entire plane, it is possible to redefine the domain box to be a rectangle once again, resulting in Figure 6.

The above discussion has summarized our basic strategy for representing FM efficiently; it now remains to concretize these notions in the framework of an arbitrary dynamical system defined by DAEs. This is accomplished in the following section by the WaMPDE, which is a partial differential equation similar to the MPDE, but with a multiplicative factor of $\frac{\partial \phi}{\partial t}$ modifying one of the differential terms. By solving the WaMPDE together with the phase condition mentioned above, compact representations of the solutions of autonomous systems can be found by efficient numerical methods.

4 The Warped Multirate Partial Differential Equation (WaMPDE)

We consider a nonlinear system modelled using vector differential-algebraic equations (DAEs), a description adequate for circuits [CL75] and many other applications:

$$\frac{d}{dt} q(x(t)) + f(x(t)) = b(t) \qquad (12)$$

In the circuit context, $x(t)$ is a vector of node voltages and branch currents; $q()$ and $f()$ are nonlinear functions describing the charge/flux and resistive terms, respectively. $b(t)$ is a vector forcing term consisting of inputs, usually independent voltage or current sources.

We now define the $(p+1)$-dimensional WaMPDE to be

$$\sum_{i=1}^{p} \left(\omega_i(\tau_{p+1}) \frac{\partial q(\hat{x})}{\partial \tau_i} \right) + \frac{\partial q(\hat{x})}{\partial \tau_{p+1}} + f(\hat{x}) = \hat{b}(\tau_1, \cdots, \tau_{p+1}). \qquad (13)$$

$\tau_1, \cdots, \tau_p$ are p warped time scales, while τ_{p+1} is an unwarped time scale. Each warped time variable has an associated frequency function $\omega_i(\tau_{p+1})$, which depends on the unwarped time variable. $\hat{x}$ and $\hat{b}$ are multivariate functions of the $p+1$ time variables. These quantities represent generalizations of the concepts introduced in Section 3 – each warped time corresponds to an independent FM mode of the system, while the unwarped one represents a non-FM time scale. It is straightforward to extend (13) to more than one unwarped time scale.

The utility of (13) lies in its special relationship with (12). Consider any solution $\hat{x}$ of (13), together with the condition

$$b(t) = \hat{b}(\phi_1(t), \cdots, \phi_p(t), t), \quad \phi_i(t) = \int_0^t \omega_i(\tau) \, d\tau. \qquad (14)$$

If we define the function $x(t)$ as

$$x(t) = \hat{x}(\phi_1(t), \cdots, \phi_p(t), t), \qquad (15)$$

then one can show by substitution that $x(t)$ satisfies (12). Hence, if we can find any solution of (13), we have automatically found one for the original problem, i.e., (12). As explained in Section 3, solving the WaMPDE directly for the multivariate functions can be advantageous.

For concreteness in the following, we now specialize to the case when there are only two time variables, and the function b is used directly in (13):

$$\omega(\tau_2) \frac{\partial q(\hat{x})}{\partial \tau_1} + \frac{\partial q(\hat{x})}{\partial \tau_2} + f(\hat{x}(\tau_1, \tau_2)) = b(\tau_2). \qquad (16)$$

Corresponding to (14) and (15), specifying

$$x(t) = \hat{x}(\phi(t), t), \quad \phi(t) = \int_0^t \omega(\tau_2) \, d\tau_2 \qquad (17)$$

results in $x(t)$ being a solution to (12).

Next, we describe how (16) can be solved to determine $\hat{x}(\tau_1, \tau_2)$ and $\omega(\tau_2)$. We first assume that $\hat{x}(\tau_1, \tau_2)$ is periodic in τ_1 with period 1:

$$\hat{x}(\tau_1, \tau_2) = \sum_{i=-\infty}^{\infty} \hat{X}_i(\tau_2) e^{ji\tau_1} \qquad (18)$$

We note that if $\hat{x}(\tau_1, \tau_2)$ satisfies (16), then so does for $\hat{x}(\tau_1 + \Delta, \tau_2)$, for any $\Delta \in R$ – this is simply because (16) is autonomous in the τ_1 time scale. We remove this ambiguity in the same way as for unforced autonomous systems, i.e., by fixing the phase of (say) the kth variable to some value,[3] e.g., 0. This is the phase constraint mentioned in Section 3.

We expand (16) in one-dimensional Fourier series in τ_1, and also include the phase constraint, to obtain:

$$\sum_{i=-\infty}^{\infty} \left(\frac{\partial \hat{Q}_i(\tau_2)}{\partial \tau_2} + ji\omega(\tau_2)\hat{Q}_i(\tau_2) + \hat{F}_i(\tau_2) \right) e^{ji\tau_1} = b(\tau_2) \qquad (19)$$

$$\Im \left\{ \hat{X}_l^k(\tau_2) \right\} = 0 \qquad (20)$$

$\hat{Q}_i(\tau_2)$ and $\hat{F}_i(\tau_2)$ are the Fourier coefficients of $q(\hat{x}(\tau_1, \tau_2))$ and $f(\hat{x}(\tau_1, \tau_2))$, respectively. k and l are fixed integers; $\hat{X}_l^k(\tau_2)$ denotes the lth Fourier coefficient of the kth element of $\hat{x}$.

(19) and (20) together form a DAE system which can be solved for isolated solutions. In practice, the Fourier series (19) can be truncated to $N_0 = 2M + 1$ terms with i restricted to $-M, \cdots, M$. In this case, (19) and (20) lead to $N_0 + 1$ equations in the same number of unknown functions of τ_2.

Applying periodic or initial boundary conditions to the DAE system (19) and (20) leads to quasiperiodic or envelope-modulated FM solutions, and also captures other interesting phenomena like mode locking and period multiplication. First, we consider periodic boundary conditions.

4.1 Quasiperiodic and envelope solutions

Assume $b(t)$ periodic with period T_2 or angular frequency $\omega_2 = \frac{2\pi}{T_2}$. Also assume that the solution of (16) is periodic in both arguments, i.e., $\hat{x}(\tau_1, \tau_2)$ is $(1, T_2)$-periodic and $\omega(\tau_2)$ is T_2-periodic. $\omega(\tau_2)$ can then be written as:

$$\omega(\tau_2) = \omega_0 + p'(\tau_2) \qquad (21)$$

where ω_0 is a constant and $p'(\cdot)$ is a zero-mean T_2-periodic waveform. Using (21) and (17), we obtain an expression for ϕ:

$$\phi(t) = \omega_0 t + p(t) \qquad (22)$$

where $p(t)$ is a T_2-periodic function.

We motivate these assumptions by showing that such periodic forms for $\hat{x}(\cdot, \cdot)$ and $\omega(\cdot)$ capture FM- and AM-quasiperiodicity, mode-locking and period multiplication.

Expand $\hat{x}(\tau_1, \tau_2)$ in Fourier series:

$$\hat{x}(\tau_1, \tau_2) = \sum_{i,k=-\infty}^{\infty} \hat{X}_{i,k} e^{ji\tau_1} e^{jk\omega_2\tau_2} \qquad (23)$$

where the constants $\hat{X}_{i,k}$ are Fourier coefficients. Substituting (23) into (17), we obtain:

$$x(t) = \sum_{i,k=-\infty}^{\infty} \hat{X}_{i,k} e^{ji(\omega_0 t + p(t))} e^{jk\omega_2 t} \qquad (24)$$

Consider, for example, the term of (24) with $i = 1$ and $k = 0$:

$$\hat{X}_{1,0} e^{j(\omega_0 t + p(t))} = \hat{X}_{1,0} \cos(\omega_0 t + p(t)) + j\hat{X}_{1,0} \sin(\omega_0 t + p(t)) \quad (25)$$

When $\omega(t)$ is nontrivially T_2-periodic, $p(t)$ is also nontrivially T_2-periodic. (25) can then readily be recognized to be a frequency-modulated signal with instantaneous frequency $\omega(t)$. Hence the WaMPDE with periodic solutions can capture not only FM signals, but also the more general form of (24).

We now show that various special cases of $\omega(\cdot)$ correspond to physical situations of interest. When $\omega(\cdot)$ is simply some constant ω_0, i.e.,

---

[3]or some slow function of τ_2; the selection of a slowly-varying phase condition is, in fact, the key to compact numerical representation of $\hat{x}(\cdot, \cdot)$.

$p'(\cdot) \equiv 0$, then the time-domain solution (24) has no frequency modulation, but is AM-quasiperiodic with angular frequencies ω_0 and ω_2. If $\omega_0 = \omega_2$, the response has the same period as the external forcing frequency, and the system is mode-locked or entrained. If ω_0 is a submultiple of ω_2, the period of the response is a multiple of that of the forcing. This phenomenon, period multiplication, is not only often designed for (e.g., in frequency dividing circuits), but is also observed in dynamic systems en route to chaos.

Next, we indicate how (19) and (20), with periodic boundary conditions, can be turned into a set of nonlinear equations for numerical solution[4]. (19) and (20) is discretized at N_1 points along the τ_2 axis, covering the interval $[0, T_1]$. The differentiation operator is replaced by a numerical differentiation formula (e.g., Backward Euler or Trapezoidal), and when the periodic boundary condition $\hat{X}_i(0) = \hat{X}_i(T_1)$ is applied, a system of $N_1(N_0 + 1)$ nonlinear algebraic equations in $N_1(N_0 + 1)$ unknowns is obtained. This set of equations is solved with any numerical method for nonlinear equations, such as Newton-Raphson or continuation, to obtain the solution of the WaMPDE. Further, when iterative linear algebra and factored-matrix methods are employed, computation and memory requirements grow almost linearly with size, making calculations practical for even large systems.

By applying initial conditions rather than periodic boundary conditions, (19) and (20) can be solved for aperiodic $\left(\{\hat{X}_i(\tau_2)\}, \omega(\tau_2)\right)$. These envelope-modulated solutions can be useful for investigating transient behaviour in systems with FM. To obtain envelope solutions, (19) and (20) are solved by time-stepping in τ_2 using any DAE solution method, starting from (say) $\tau_2 = 0$. An initial condition $\left(\{\hat{X}_i(0)\}, \omega(0)\right)$ is specified. For typical applications, a natural initial condition is the solution of (12) with no forcing, *i.e.*, with $b(t)$ constant. The procedure for discretizing of the WaMPDE for quasiperiodic or time-stepping solutions is similar to that for the MPDE; further details may be found in [Roy99].

5   Applications

A voltage-controlled oscillator (VCO) was simulated using the new WaMPDE-based numerical techniques. The oscillator consisted of an LC tank in parallel with a nonlinear resistor, whose resistance was negative in a region about zero and positive elsewhere. This led to a stable limit cycle. The capacitance was varied by adjusting the physical plate separation of a novel MEMS (**M**icro **E**lectro**M**echanical **S**tructure) varactor with a separate control voltage. The damping parameter of the mechanical structure was initially assumed small, corresponding to a near vacuum.
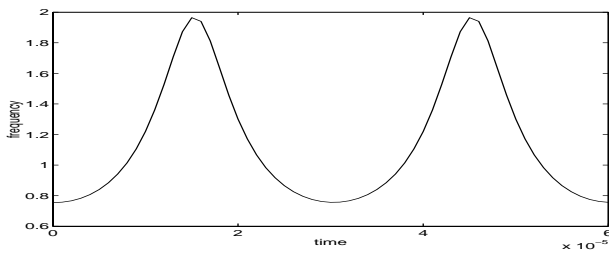
Figure 7: VCO: frequency modulation

An envelope simulation was conducted using purely time-domain numerical techniques for both τ_1 and τ_2 axes. The initial control voltage of 1.5V resulted in an initial frequency of about 0.75MHz; the control voltage was then varied sinusoidally with time-period 30 times that of the unforced oscillator. Figure 7 shows the resulting change in local frequency, which varies by a factor of almost 3.

Figure 8 depicts the bivariate waveform of the capacitor voltage (*i.e.*, one entry of the vector $\hat{x}(\tau_1, \tau_2)$, with the warped τ_1 axis scaled to the oscillator's nominal time-period of $1\mu s$). It is seen that the controlling voltage changes not only the local frequency, but also the amplitude and shape of the oscillator waveform.

The circuit was also simulated by traditional numerical ODE methods ("transient simulation"). The waveform from this simulation, together with the 1-dimensional waveform obtained by applying (15)

---

[4]We outline a time-domain method for the τ_2 axis, leading to a mixed frequency-time method; purely time-domain or frequency-domain methods are equally straightforward.
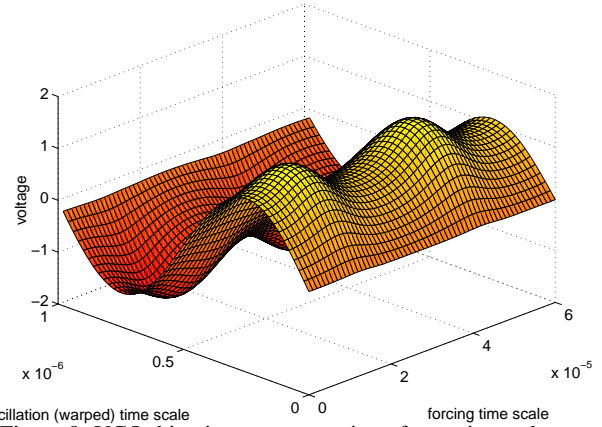
Figure 8: VCO: bivariate representation of capacitor voltage

to Figure 8, are shown in Figure 9. The match is so close that it is difficult to tell the two waveforms apart; however, the thickening of the lines at about $60\mu s$ indicates a deviation of the transient result from the WaMPDE solution. Frequency modulation can be observed in the varying density of the undulations.
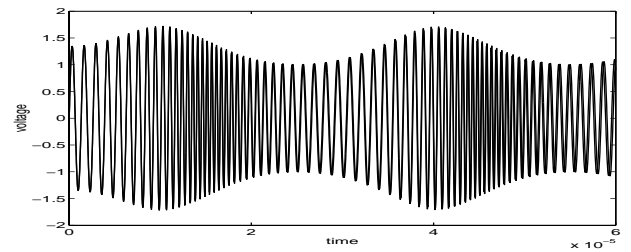
Figure 9: VCO: WaMPDE vs transient simulation

The VCO was simulated again after two modifications: the damping of the MEMS varactor was increased to correspond to an air-filled cavity, and the controlling voltage was varied much more slowly, *i.e.*, about 1000 times slower than the nominal period of the oscillator. The controlling voltage remained sinusoidal but with a period of 1ms. Figure 10 shows the new variation in frequency; note the settling behaviour and the smaller change in frequency, both due to the slow dynamics of the air-filled varactor.
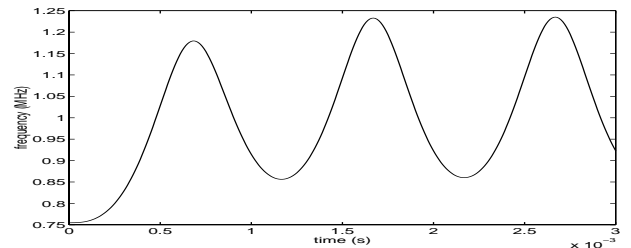
Figure 10: Modified VCO: frequency modulation

Figure 11 depicts the new bivariate capacitor voltage waveform. Note that unlike Figure 8, the amplitude of the oscillation changes very little with the forcing. This was corroborated by transient simulation, the full results of which are not depicted due to the density of the fast oscillations. A small section of the one-dimensional waveform, consisting of a few cycles around 0.3ms, is shown in Figure 12. The one-dimensional WaMPDE output of (14) is compared against two runs of direct transient simulation, using 50 and 100 points per nominal oscillation period, respectively. It can be seen that even at an early stage of the simulation, direct transient simulation with 50 points per cycle builds up significant phase error. This is reduced considerably when 100 points are taken per cycle, but further along (not shown), the error accumulates again, reaching many multiples of 2π by the end of the

simulation at 3ms. In contrast, the WaMPDE achieves much tighter control on phase because the phase condition (a time-domain equivalent of (20)) explicitly prevents build-up of error. To achieve accuracy comparable to the WaMPDE, transient simulation required 1000 points per nominal cycle, with a resulting speed disadvantage of two orders of magnitude.
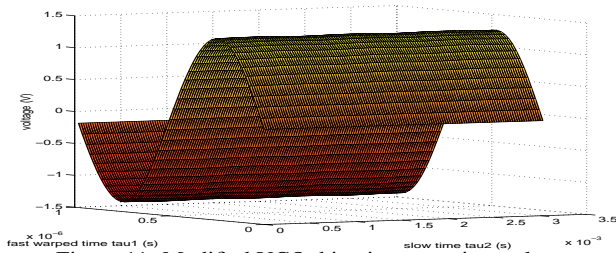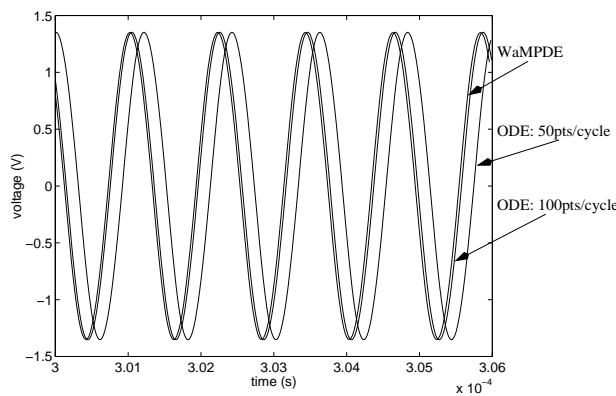

Figure 11: Modified VCO: bivariate capacitor voltage

Figure 12: Modified VCO: WaMPDE vs transient (a few cycles at 10% of the full run; phase errors from transient increase later)

6 Conclusion

We have presented a new, efficient, approach for analysing the dynamics of oscillatory systems. The approach uses multiple time scales and time warping functions to obtain a partial differential formulation (the WaMPDE) for autonomous dynamical systems. Solving the WaMPDE by efficient numerical methods enables us to predict complex phenomena, such as frequency modulation, in large autonomous systems quickly and accurately. We have extended the notion of instantaneous frequency to general settings and provided methods for calculating it explicitly. We have applied our methods to VCO circuits and shown that they have significant speed and accuracy advantages over previously existing techniques.

Acknowledgments

References

[AT72]   T.J. Aprille and T.N. Trick. Steady-state analysis of nonlinear circuits with periodic inputs. *Proc. IEEE*, 60(1):108–114, January 1972.

[BL98]   H.G. Brachtendorf and R. Laur. Transient Simulation of Oscillators. Technical Report ITD-98-34096K, Bell Laboratories, 1998.

[BWLBG96] H.G. Brachtendorf, G. Welsch, R. Laur, and A. Bunse-Gerstner. Numerical steady state analysis of electronic circuits driven by multi-tone signals. *Electrical Engineering (Springer-Verlag)*, 79:103–112, 1996.

[CL75]   L.O. Chua and P-M. Lin. *Computer-aided analysis of electronic circuits : algorithms and computational techniques*. Prentice-Hall, Englewood Cliffs, N.J., 1975.

[Far94]   M. Farkas. *Periodic Motions*. Springer-Verlag, 1994.

[Got97]   I.M. Gottlieb. *Practical oscillator handbook*. Oxford, 1997.

[GS91]   R.J. Gilmore and M.B. Steer. Nonlinear circuit analysis using the method of harmonic balance – a review of the art. Part I. Introductory concepts. *Int. J. on Microwave and Millimeter Wave CAE*, 1(1), 1991.

[Haa88]   S.A. Haas. *Nonlinear Microwave Circuits*. Artech House, Norwood, MA, 1988.

[Hay64]   C. Hayashi. *Nonlinear Oscillations in Physical Systems*. McGraw-Hill, 1964.

[KC81]   J. Kevorkian and J.D. Cole. *Perturbation methods in Applied Mathematics*. Springer-Verlag, 1981.

[Lor63]   E.N. Lorenz. Deterministic nonperiodic flow. *J. Atmos. Sci*, 20:130–141, 1963.

[Mar92]   Markus Rösch. *Schnell Simulation des stationären Verhaltens nichtlinearer Schaltungen*. PhD thesis, Technischen Universität München, 1992.

[MFR95]   R.C. Melville, P. Feldmann, and J. Roychowdhury. Efficient multi-tone distortion analysis of analog integrated circuits. In *Proc. IEEE CICC*, pages 241–244, May 1995.

[Mur91]   J.A. Murdock. *Perturbations: Theory and Methods*. Wiley, 1991.

[NB95]   A. Nayfeh and B. Balachandran. *Applied Nonlinear Dynamics*. Wiley, 1995.

[NV76]   M.S. Nakhla and J. Vlach. A Piecewise Harmonic Balance Technique for Determination of Periodic Responses of Nonlinear Systems. *IEEE Trans. Ckts. Syst.*, CAS-23:85, 1976.

[Par83]   B. Parzen. *Design of crystal and other harmonic oscillators*. Wiley, 1983.

[PC89]   T.S. Parker and L.O. Chua. *Practical Numerical Algorithms for Chaotic Systems*. Springer-Verlag, 1989.

[RN88]   V. Rizzoli and A. Neri. State of the Art and Present Trends in Nonlinear Microwave CAD Techniques. *IEEE Trans. MTT*, 36(2):343–365, February 1988.

[Roh97]   U. Rohde. *Microwave and wireless synthesizers: theory and design*. Wiley, 1997.

[Roy97]   J. Roychowdhury. Efficient Methods for Simulating Highly Nonlinear Multi-Rate Circuits. In *Proc. IEEE DAC*, 1997.

[Roy99]   J. Roychowdhury. Analysing Circuits with Widely-Separated Time Scales using Numerical PDE Methods. *IEEE Trans. Ckts. Syst. – I: Fund. Th. Appl.*, May 1999.

[Saa96]   Y. Saad. *Iterative methods for sparse linear systems*. PWS, Boston, 1996.

[Ske80]   S. Skelboe. Computation of the periodic steady-state response of nonlinear networks by extrapolation methods. *IEEE Trans. Ckts. Syst.*, CAS-27(3):161–175, March 1980.

[TKW95]   R. Telichevesky, K. Kundert, and J. White. Efficient Steady-State Analysis based on Matrix-Free Krylov Subspace Methods. In *Proc. IEEE DAC*, pages 480–484, 1995.

[vdP22]   B. van der Pol. On oscillation hysteresis in a simple triode generator. *Phil. Mag.*, 43:700–719, 1922.

[Ven82]   G.D. Vendelin. *Design of amplifiers and oscillators by the S-parameter method*. Wiley, 1982.